

Endocytosis and Vacuolar Degradation of the Yeast Cell Surface Glucose Sensors Rgt2 and Snf3*

Received for publication, December 2, 2013, and in revised form, January 14, 2014. Published, JBC Papers in Press, January 22, 2014, DOI 10.1074/jbc.M113.539411

Adhiraj Roy and Jeong-Ho Kim¹

From the Department of Biochemistry and Molecular Medicine, George Washington University Medical Center, Washington, D.C. 20037

Background: In yeast, glucose is sensed by two cell surface glucose sensors.

Results: The glucose sensors are down-regulated by ubiquitination and degradation.

Conclusion: The stability of the glucose sensors may be associated with their ability to sense glucose.

Significance: Differential regulation of the abundance of glucose sensors enables yeast cells to respond rapidly to changing glucose levels.

Sensing and signaling the presence of extracellular glucose is crucial for the yeast *Saccharomyces cerevisiae* because of its fermentative metabolism, characterized by high glucose flux through glycolysis. The yeast senses glucose through the cell surface glucose sensors Rgt2 and Snf3, which serve as glucose receptors that generate the signal for induction of genes involved in glucose uptake and metabolism. Rgt2 and Snf3

myces cerevisiae, because regulation of cellular function by glucose dictates the fermentative lifestyle of the organism (3, 4). The propensity of the yeast to ferment rather than oxidize glucose demands high glycolytic flux, and therefore, yeast cells consume the available glucose vigorously by increasing glucose uptake through glucose transporters (HXTs) (3, 5).

Expression of the HXT genes is repressed in the absence of

WITHDRAWN
June 14, 2016

This article has been withdrawn by the authors. The actin immunoblot from the WT strain in Fig. 2C was reused as the actin immunoblot from the *end3Δ* strain in Fig. 2C and as the actin immunoblot in the *right panel* of Fig. 2D. The HA immunoblot in Fig. 3D was assembled from different immunoblots and was represented as being from the same immunoblot to place them with increasing size in a single panel.

suggesting that the stability of the glucose sensors may be associated with their ability to sense glucose. Therefore, our findings demonstrate that the amount of glucose available dictates the cell surface levels of the glucose sensors and that the regulation of glucose sensors by glucose concentration may enable yeast cells to maintain glucose sensing activity at the cell surface over a wide range of glucose concentrations.

Most organisms have evolved numerous mechanisms for sensing and signaling the availability of glucose, the universal fuel for life, ensuring its optimal utilization (1, 2). Glucose is by far the preferred energy source of the budding yeast *Saccharo-*

glucose into the cell; instead, they function as glucose receptors (20, 21). This view is strongly supported by the identification of a dominant mutation in the glucose sensor genes (*RGT2-1* and *SNF3-1*), which is thought to convert the sensors into the glucose-bound and therefore glucose signaling forms (20). Indeed, Mth1 degradation and subsequent *HXT* gene expression occur constitutively in Rgt2-1 and Snf3-1 mutant cells (22). These observations have led to the view that glucose acts like a hormone to initiate receptor-mediated signaling, and glucose sensors function in a similar way to mammalian cell surface receptors (5, 23).

The yeast cells possess multiple glucose transporters with different affinities for glucose, enabling them to grow well over a wide range of glucose concentrations, from a few micromolar to a few molar (3). They sense extracellular glucose levels through the two glucose sensors, which have different affinities for glucose. Rgt2 has a low affinity for glucose, and Snf3 has a high affinity for glucose (21). This difference is presumably due to differences in the amino acid residues of the sensors that

* This work was supported, in whole or in part, by National Institutes of Health Grant GM087470 (to J.-H. K.).

¹ To whom correspondence should be addressed: Dept. of Biochemistry and Molecular Medicine, George Washington University Medical Center, 2300 Eye St., Washington, D.C. 20037. Tel.: 202-994-9937; Fax: 202-994-8974; E-mail: jh_kim@gwu.edu.

TABLE 1

Yeast strains used in this study

Strain	Genotype	Source
BY4741	<i>Mata his3Δ1 leu2Δ0 ura3Δ0 met15Δ</i>	Ref. 28
YM6870	<i>Mata his3Δ1 leu2Δ0 ura3Δ0 met15Δ rgt2::KanMX snf3::KanMX</i>	Ref. 28
KFY122	<i>Mata his3Δ1 leu2Δ0 lys2Δ0 ura3Δ0 doa4::KanMX</i>	This study
KFY123	<i>Mata his3-1 leu2-0 ura3-0 RSP5</i>	Ref. 35
KFY124	<i>Mata his3-1 leu2-0 ura3-0 rsp5-1/smm1</i>	Ref. 35
KFY127	<i>Mata his3Δ1 leu2Δ0 lys2Δ0 ura3Δ0 end3::KanMX</i>	This study
KFY128	<i>Mata his3Δ1 leu2Δ0 lys2Δ0 ura3Δ0 pep4::KanMX</i>	This study
JKY88	<i>Mata his3Δ1 leu2Δ0 ura3Δ0 met15Δ LYS2 pHXT1-NAT</i>	Ref. 36
JKY89	<i>Mata his3Δ1 leu2Δ0 ura3Δ0 met15Δ LYS2 pHXT2-NAT</i>	Ref. 36

form the glucose-binding site. Thus, it has been proposed that Rgt2 functions as a low affinity glucose receptor that senses high concentrations of glucose, whereas Snf3 serves as a high affinity glucose receptor that senses low levels of glucose (20, 21). However, it remains unknown whether the abundance and function of cell surface levels of the glucose sensors are associated with their affinity for glucose and thus affect glucose signaling.

Here, we provide evidence that cell surface levels of glucose sensors are regulated by ubiquitination and degradation in the vacuole. Our results indicate that the stability of glucose sensors are correlated with their affinity for glucose and that the constitutively active, signaling forms of glucose sensor mutants are stable against degradation. These observations suggest that the conformation of the glucose sensors is critical for their stability. We discuss the biological significance of this observation from the perspective of the fermentative metabolism of glucose, regulated by high glucose uptake and increased

EXPERIMENTAL PROCEDURES

Yeast Strains—The *S. cerevisiae* strains used in this study are listed in Table 1. Cells were grown in YEA (yeast extract) and SC (synthetic complete) media (Sigma) containing 0.17% yeast nitrogen base (Sigma) and 0.5% yeast extract (Sigma) media supplemented with the appropriate amino acids and carbon sources.

Plasmid Construction—The plasmids used in this study are listed in Table 2. The plasmids were constructed by using standard molecular biology techniques as described below. Plasmids containing Rgt2-HA, Rgt2 (1–545)-HA, Rgt2 (1–620)-HA, Rgt2 (1–720)-HA, and Rgt2-1-HA under its endogenous promoter (1000 base pairs) were constructed in two steps. First, the promoter element was PCR-amplified from genomic DNA isolated from wild type yeast strain as a EcoRI-BamHI fragment and cloned in the empty HA vector (KFP 69, C-terminal 3 × HA fusion vector). Next, the RGT2 ORFs were fused as BamHI-XbaI fragments after the promoter region. Plasmids containing Rgt2^{K637A}-HA, Rgt2^{K657A}-HA, Rgt2^{K637,657A}-HA, Rgt2^{W529F}-HA, and Rgt2^{W529Y}-HA were constructed by QuikChange site-directed mutagenesis kit (Stratagene) according to the manufacturer's protocol. Plasmids containing GFP-Rgt2 and GFP-Rgt2-1 were constructed by fusing RGT2 and RGT2-1 ORFs as a BamHI-XhoI fragment in pUG34 vector. Plasmids containing Snf3-HA and Snf3-1-HA under its endogenous promoter (1000 base pairs) were constructed in two steps. First, the promoter element was PCR-amplified from genomic DNA isolated from

TABLE 2

Plasmids used in this study

Plasmid	Description	Source
KFP69	pAD80, 3 × HA-CYC1 terminator, Leu2	Ref. 10
JKP253	pAD80-P _{RGT2} -Rgt2-3 × HA	This study
JKP252	pAD80-P _{RGT2} -Rgt2 (1–545)-3 × HA	This study
JKP299	pAD80-P _{RGT2} -Rgt2 (1–620)-3 × HA	This study
JKP300	pAD80-P _{RGT2} -Rgt2 (1–720)-3 × HA	This study
JKP301	pAD80-P _{RGT2} -Rgt2 (K637A)-3 × HA	This study
JKP302	pAD80-P _{RGT2} -Rgt2 (K657A)-3 × HA	This study
JKP308	pAD80-P _{RGT2} -Rgt2 (K637A, K657A)-3 × HA	This study
JKP303	pAD80-P _{RGT2} -Rgt2 (W529Y)-3 × HA	This study
JKP304	pAD80-P _{RGT2} -Rgt2 (W529F)-3 × HA	This study
JKP295	pAD80-P _{RGT2} -Rgt2 (1–3 × HA	This study
JKP298	pAD80-P _{RGT2} -Rgt2 (1–3 × HA	This study
JKP311	pAD80-P _{RGT2} -Rgt2 (1–3 × HA	This study
pBAM	pBAM, 3 × HA-CYC1 terminator, His3	Ref. 17
JKP305	pAD80-P _{RGT2} -Rgt2 (1–3 × HA	This study
JKP306	pAD80-P _{RGT2} -Rgt2 (1–3 × HA	This study
JKP307	pAD80-P _{RGT2} -Rgt2 (1–3 × HA	This study

from genomic DNA isolated from wild type yeast strain as a SacI-XbaI fragment cloned in the empty HA vector (KFP69). Then SNF3 and SNF3-1 ORFs were fused as XbaI-SphI fragments. Plasmids containing GFP-Snf3 and GFP-Snf3-1 were constructed by “gap repair” of BamHI-EcoRI linearized pUG34 vector (17).

Yeast Membrane Preparation and Western Blotting—Membrane-enriched fractions were essentially prepared as described previously (24). Briefly, after washing with phosphate buffer, pH 7.4, containing 10 mM sodium azide, the cell pellet was resuspended in ice-cold membrane isolation buffer (100 mM Tris-Cl, pH 8, 150 mM NaCl, 5 mM EDTA) containing 10 mM sodium azide, protease, and phosphatase inhibitors and vortexed with acid-washed glass beads. After diluting the samples with the same buffer, unbroken cells and debris were removed by centrifugation, and the membrane-enriched fraction was collected by centrifuging the samples at 12,000 rpm for 40 min at 4 °C. The pellets were resuspended in the aforementioned buffer containing 5 M urea and incubated for 30 min on ice and further centrifuged at 12,000 rpm for 40 min at 4 °C. The proteins were precipitated with 10% TCA, neutralized with 20 μl of 1 M Tris base, and finally dissolved in 80 μl of SDS buffer (50 mM Tris-HCl, pH, 6.8, 10% glycerol, 2% SDS, 5% β-mercaptoethanol).

For Western blotting, proteins were resolved by 10% SDS-PAGE and transferred to PVDF membrane (Millipore), and the membranes were incubated with appropriate antibodies (anti-HA, anti-Myc, anti-GFP, or anti-actin antibody; Santa Cruz) in TBST buffer (10 mM Tris-HCl, pH, 7.5, 150 mM NaCl, 0.1% Tween 20), and proteins were detected by the ECL system (Pierce).

Quantitative RT-PCR—Total RNA was extracted by RNeasy mini kit (Qiagen) following manufacturer's protocol, and 2 μ g of total RNA was converted to cDNA by qScript cDNA supermix (Quanta Biosciences). cDNA was analyzed by qRT-PCR² using SsoFast Evagreen reagent (Bio-Rad) in CFX96 real time thermal cycler (Bio-Rad). *ACT1* was used as an internal control to normalize expression of *HXT1*, *RGT2*, and *SNF3* genes. Quantification data were the averages of three independent experiments with error bars representing standard deviation (S.D.). Statistical significance was defined by *p* values: *, *p* < 0.05, and **, *p* < 0.001 as compared with control.

Microscopy and Image Analysis—To visualize yeast cells expressing various GFP fusion proteins, cells were stained with FM4-64 (lipophilic styryl dye for selectively staining vacuolar membrane, 5 mg/ml stock in DMSO) and examined with Olympus FluoView confocal microscope under 63 \times oil immersion objective lens using GFP and Texas Red filters. Images from confocal microscope were captured by FluoView software (Olympus), and National Institutes of Health ImageJ v1.4r software was used to quantify fluorescence intensities from unmanipulated raw images. Regions of interest in the plasma or vacuolar membrane and an area outside the cell (background) were traced using the free-hand tool, and mean fluorescence intensities (both GFP and FM4-64) were measured. After background subtraction, the GFP signals in the plasma membrane were normalized to the FM4-64 signal of vacuolar membrane. At least 50 cells were counted, and the data represent the averages with error bars representing S.D.

RESULTS

Glucose Starvation Induces Endocytosis and Degradation of Rgt2—To test the hypothesis that the levels of Rgt2 glucose sensor may be regulated by glucose concentration, we determined its expression levels in cells grown in different glucose concentrations. Confocal microscopy analysis showed that the cell surface levels of Rgt2-HA are greater in high glucose-grown cells (2%) than in cells grown in low glucose medium (\sim 0.1%) and are very low in cells grown in the absence of glucose (Gal) (Fig. 1A). However, *RGT2* mRNA levels were not significantly different between yeast cells incubated with different concentrations of glucose (Fig. 1B), and the treatment of the protein synthesis inhibitor cycloheximide did not greatly affect Rgt2 turnover (Fig. 1C).

Because a number of yeast plasma membrane receptors and transporters are down-regulated by endocytosis and degradation in the vacuole (25, 26), we examined expression levels of Rgt2-HA in the *end3 Δ* mutant defective in the internalization step of endocytosis and the *pep4 Δ* mutant defective in vacuolar protease processing. Rgt2-HA levels in glucose-grown wild type cells were reduced by \sim 50% within 20 min after the cells were shifted to glucose-depleted (galactose) medium, but this reduction was not observed in the *end3 Δ* and *pep4 Δ* strains (Fig. 1D). Consistently, the amount of immunodetected Rgt2-HA was markedly increased within 30 min after addition of glucose to glucose-starved medium (Fig. 1E).

Confocal microscopy demonstrated that GFP-Rgt2 is present at the cell surface in glucose-grown cells and that \sim 80% of GFP-Rgt2 is removed from there when the yeast cells are shifted from glucose to galactose medium (Fig. 1F, WT). However, GFP-Rgt2 was constitutively detected at the cell surface of the *end3 Δ* mutant (Fig. 1F) and the *pep4 Δ* mutant (data not shown). It was also shown that substantial amounts of GFP-Rgt2 were localized to the vacuole in a glucose-independent manner, suggesting constitutive internalization and degradation of Rgt2 (Fig. 1F, FM4-64). Glucose and galactose only differ with respect to C-4, yet galactose does not activate the glucose sensors, suggesting that the glucose sensors display remarkable substrate specificity (27). Consistently, we found that Rgt2-HA levels are down-regulated in the cells grown on galactose, raffinose, or ethanol (Fig. 1G). These data indicate that Rgt2 is stable against degradation in the presence of high concentrations of glucose but endocytosed and degraded in the vacuole when glucose is absent or present only in small quantities.

Snf3 Expression Is Regulated at Both Transcriptional and Post-translational Levels—Given that glucose starvation induces endocytosis and degradation of Rgt2, we determined whether Snf3 is also regulated by glucose concentration. Confocal microscopy showed that the plasma membrane levels of Snf3-HA are higher in high glucose-grown cells than in low glucose-grown cells (Fig. 2A). Because *SNF3* gene expression is regulated by glucose concentration (22), we then examined whether Snf3 abundance is regulated both at the transcriptional and post-translational levels. To this end, we expressed GFP-Snf3 under the *P_{GLC1}* or *P_{MET25}* promoter, which is not regulated by glucose concentration (22). Therefore, changes of GFP-Snf3 levels in response to different glucose concentrations may be not due to transcriptional regulation but rather due to post-translational regulation. The cell surface levels of GFP-Snf3 were low in both glucose-starved and high glucose-grown cells but were high in cells grown on low glucose. In contrast, GFP-Snf3 levels were constitutively high in the *end3 Δ* mutant, suggesting Snf3 degradation via endocytosis (Fig. 2C).

The transcriptional and post-translational regulation of Snf3 expression was recapitulated in cells grown on different carbon sources. Both Snf3-HA and GFP-Snf3 levels were low in high glucose-grown cells (Glu) but high in cells grown on raffinose (Fig. 2D, Raf). Raffinose is a trisaccharide, consisting of fructose-glucose-galactose, that is equivalent to low glucose, because *S. cerevisiae* can only inefficiently cleave the fructose-glucose bond and thus obtain only low levels of fructose from it (3). Of note, GFP-Snf3, unlike Snf3-HA, was present at low levels in glucose-depleted cells, suggesting glucose depletion-induced Snf3 degradation (Fig. 2D, galactose (Gal) and ethanol (EtOH)-grown cells). Consistent with these observations, plasma membrane accumulation of GFP-Snf3 was observed only in low glucose-grown cells (Raf) but was constitutive in the *end3 Δ* mutant, suggesting that Snf3 is internalized and degraded in the vacuole of glucose-depleted cells and high glucose-grown cells (Fig. 2E). Therefore, the low affinity glucose sensor Rgt2 accumulates at the plasma membrane of the cells grown on high glucose; by contrast, the high affinity glucose sensor Snf3 accumulates in cells grown on low glucose. These

² The abbreviations used are: qRT-PCR, quantitative RT-PCR; NAT, nourseothricin.

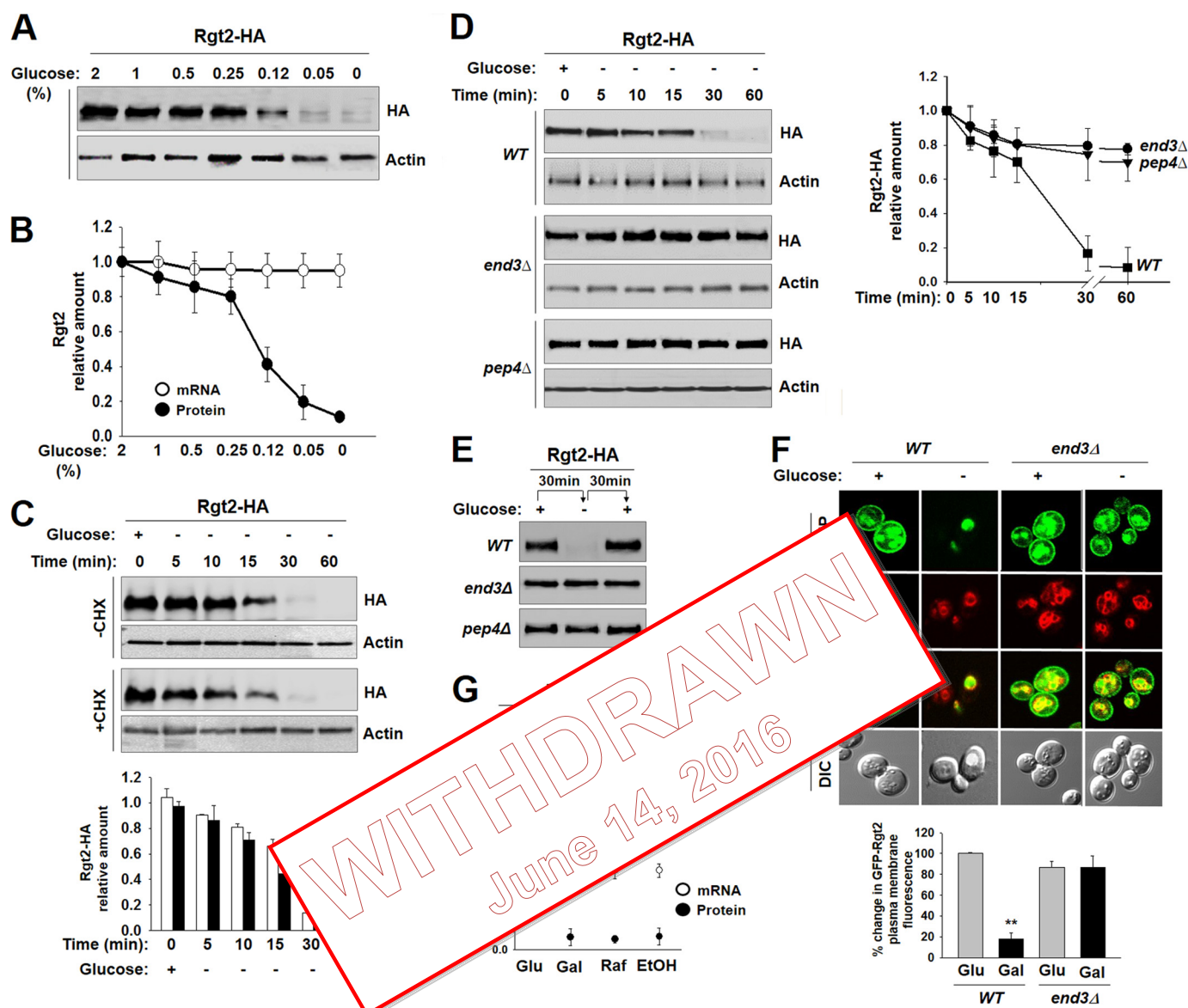


FIGURE 1. Rgt2 undergoes endocytosis and subsequent vacuolar degradation in glucose starved cells. A, Western blot analysis of Rgt2-HA levels at the plasma membrane. Yeast cells (WT) expressing Rgt2-HA were grown in SC-2% glucose medium till mid log phase ($A_{600\text{ nm}} = 1.2\text{--}1.5$), and equal amounts of cells were shifted to SC medium containing different concentrations of glucose (0–2%) for 30 min. Membrane fractions were analyzed using anti-HA antibody. B, qRT-PCR analysis of mRNA expression of *RGT2* (mRNA) in yeast cells grown as described for Fig. 1A and densitometric quantification of the intensity of each band on the blot in A (Protein). C, yeast cells (WT) expressing Rgt2-HA were grown in SC-2% glucose (+) medium till mid log phase and shifted to 2% galactose (–) medium with or without cycloheximide (CHX, 50 $\mu\text{g/ml}$) for times as indicated. Membrane fractions were immunoblotted with anti-HA antibody (top panels), and the intensity of each band on the blot was quantified by densitometric scanning (bottom panels). D, yeast cells (WT, *end3* Δ , and *pep4* Δ) expressing Rgt2-HA were grown without cycloheximide as described for C. Yeast cells were harvested at different time points as indicated, membrane fractions were immunoblotted with anti-HA antibody (left panel), and the intensity of each band on the blot was quantified by densitometric scanning (bottom panels). E, yeast cells (WT, *end3* Δ , and *pep4* Δ) expressing Rgt2-HA were grown in SC-2% glucose medium (+) till mid log phase and shifted to SC-2% galactose medium (–) for 30 min and again shifted to SC-2% glucose medium for 30 min. Membrane fractions were immunoblotted with anti-HA antibody. F, GFP-Rgt2 was expressed from the *MET25* promoter in wild type and *end3* Δ strains. Yeast cells expressing GFP-Rgt2 were grown in SC-2% glucose (+) medium till mid log phase and shifted to 2% galactose (–) medium for 30 min. Confocal microscope images (top panel) and quantification of relative GFP fluorescence in the plasma membrane (bottom panel; **, $p < 0.001$) were shown. Relative GFP fluorescence intensities were plotted with the fluorescence of WT cells (2% glucose condition) set to 100%. The data represented were averages of at least 50 cell counts with error bars representing S.D. G, yeast cells (WT) expressing Rgt2-HA were grown in SC-2% glucose (Glu) medium till mid log phase and shifted to SC medium containing either 2% galactose (Gal), 2% raffinose (Raf), or 2% ethanol (EtOH) and incubated for 30 min. Membrane fractions were immunoblotted with anti-HA antibody (top panel). qRT-PCR analysis of mRNA expression of *RGT2* (mRNA) and densitometric quantification of the intensity of each band on the blot (Protein) (bottom panel). Actin was served as a loading control in A, C, D, E, and G.

results support the view that stability of the glucose sensors is associated with their ability to sense glucose.

Rgt2 Degradation Is Ubiquitin-dependent—Ubiquitination is a signal for endocytosis of plasma membrane proteins (29, 30). The Doa4 ubiquitin isopeptidase and the Rsp5 ubiquitin ligase are known to be involved in the ubiquitination of many plasma

membrane receptors and transporters in yeast (31–34). To determine whether Rgt2 down-regulation is mediated by ubiquitination, we investigated glucose regulation of Rgt2 in the strain carrying the *doa4* Δ or *rsp5-1^{ts}* mutation (35). Rgt2-HA levels were constitutively high in both the *doa4* Δ mutant (Fig. 3A, left panels) and in the *rsp5-1^{ts}* mutant incubated at 37 $^{\circ}\text{C}$

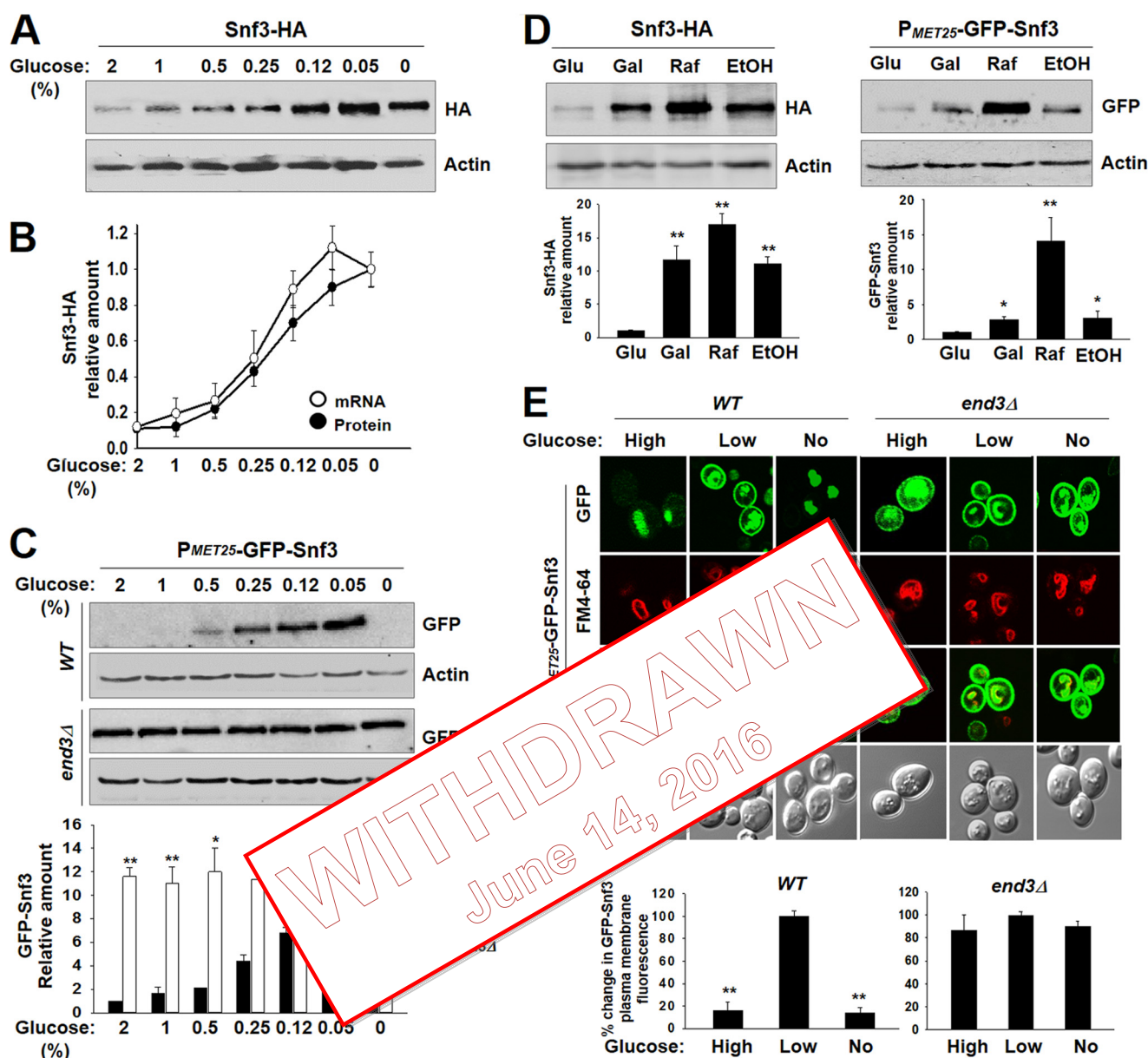


FIGURE 2. Snf3 levels are regulated by both transcriptional and translational mechanisms. A, Western blot analysis of the plasma membrane levels of Snf3-HA. Yeast cells (WT) expressing Snf3-HA were grown as described for Fig. 1A, and membrane fractions were immunoblotted with anti-HA antibody. B, qRT-PCR analysis of mRNA expression of *SNF3* (mRNA) in yeast cells grown as described for Fig. 1A and densitometric quantification of the intensity of each band on the blot in A (Protein). C, GFP-Snf3 was expressed from the *MET25* promoter in wild type and *end3Δ* strains. Yeast cells expressing GFP-Snf3 were grown as described for Fig. 1A, and membrane fractions were immunoblotted with anti-HA antibody (top panel). The intensity of each band on the blot was quantified by densitometric scanning (bottom panel; *, $p < 0.05$; **, $p < 0.001$). D, Western blot analysis of Snf3-HA and GFP-Snf3 levels at the plasma membrane. Yeast cells (WT) expressing Snf3-HA or GFP-Snf3 were grown as described for Fig. 1G. GFP-Snf3 was expressed from the *MET25* promoter. Membrane fractions were immunoblotted with anti-HA antibody (top panels), and the intensity of each band on the blot was quantified by densitometric scanning (bottom panels; *, $p < 0.05$; **, $p < 0.001$). E, GFP-Snf3 was expressed from the *MET25* promoter in wild type and *end3Δ* strains in glucose (High), raffinose (Low), or galactose (No) medium. Confocal microscope images (top panel) and quantification of relative GFP fluorescence in the plasma membrane (bottom panels; **, $p < 0.001$) were shown. Actin was served as a loading control in A, C, and D.

(Fig. 3A, right panels), compared with those in wild type cells. Consistently, GFP-Rgt2 was shown to remain stable at the plasma membrane in those mutants (Fig. 3B). To identify the ubiquitination sites in Rgt2, we constructed a series of deletion mutants of Rgt2 and used them to map the regions that are important for its stability (Fig. 3C). Rgt2 degradation is abolished by the deletion of the entire C-terminal cytoplasmic domain (residues 1–545) or significantly inhibited by the deletion of the last 143 amino acids (residues 1–620) (Fig. 3D). However, the deletion of the last 13 amino acids of Rgt2 (resi-

dues 1–720) did not affect its stability, implicating that the 100 amino acids between residues 620 and 720 that contain the two lysine residues, Lys⁶³⁷ and Lys⁶⁵⁷, may be necessary for Rgt2 ubiquitination. Indeed, substitution of the two lysine residues by alanine (K637A and K657A) markedly increased Rgt2 stability in glucose-starved cells, suggesting that the two lysine residues may serve as major ubiquitination sites (Fig. 3E).

Endocytosis-mediated degradation of Snf3 is dampened by glucose regulation of the expression of the *SNF3* gene, suggesting that Snf3 levels are mainly regulated by transcriptional con-

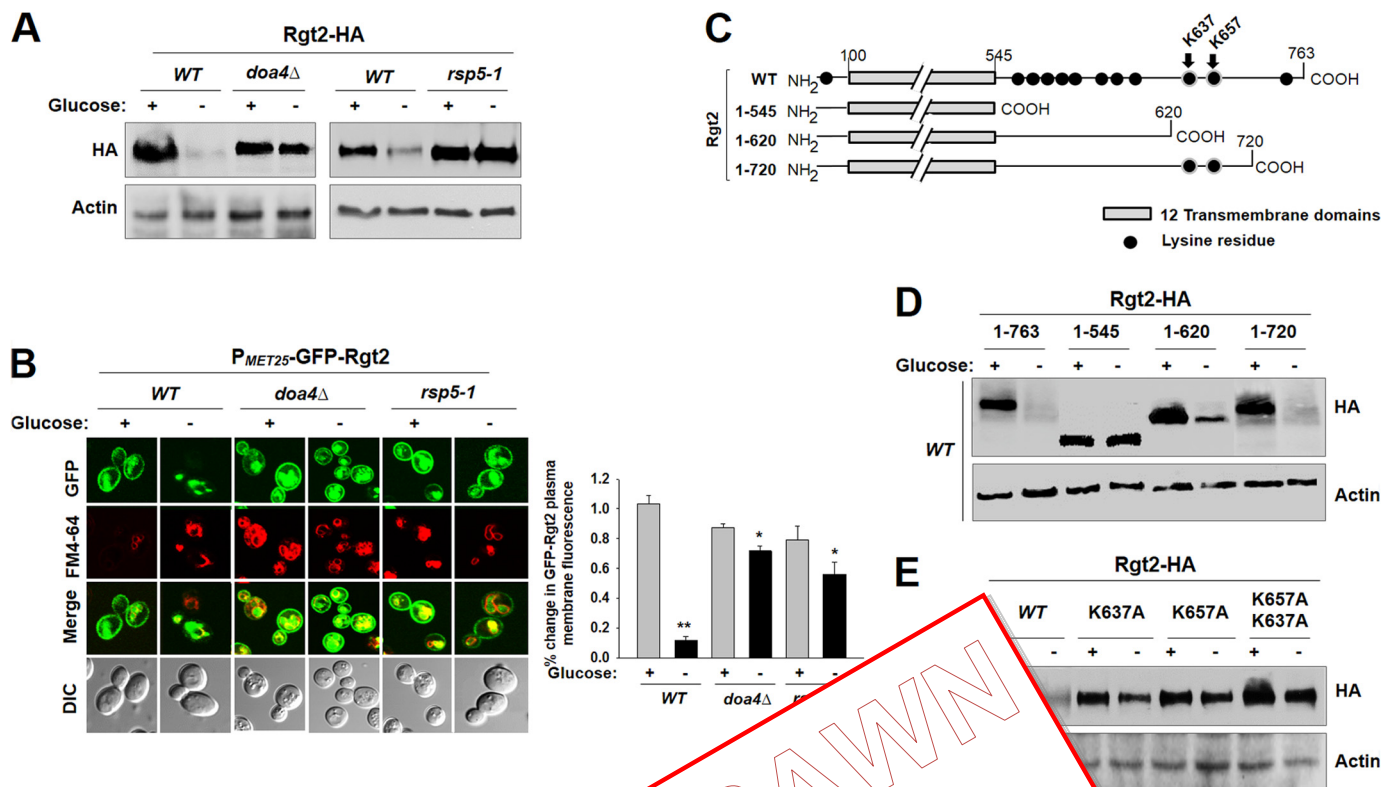


FIGURE 3. Ubiquitination of the cytoplasmic tail domain of Rgt2. A, Western blot analysis of Rgt2-HA levels at the plasma membrane. Yeast cells (WT, *doa4*Δ, and *rsp5-1*) expressing Rgt2-HA were grown in glucose (+) or galactose (-) medium, as described for Fig. 1B. The blots were immunoblotted with anti-HA antibody. B, GFP-Rgt2 was expressed from the *MET25* promoter in WT, *doa4*Δ, and *rsp5-1* strains. The cells were grown in glucose (+) or galactose (-) medium, as described for Fig. 1B. The cells were then analyzed for relative GFP fluorescence in the plasma membrane (right panel; *, *p* < 0.05; **, *p* < 0.001). C, Schematic representation of Rgt2 domain structure. The 12 transmembrane domains are shown as boxes, and the lysine residues at N- and C-terminal domains are shown as dots. The constructs used for ubiquitination analysis of Rgt2-HA levels at the plasma membrane were indicated. D and E, yeast cells (WT) expressing the indicated Rgt2-HA constructs were grown in glucose (+) or galactose (-) medium, as described for Fig. 1B. The blots were immunoblotted with anti-HA antibody.

trol. For this reason, ubiquitination of Rgt2 was examined in this study.

Constitutively Active Glucose Sensor Is Resistant against Degradation—There are dominant mutations in the glucose sensor genes (*RGT2-1* and *SNF3-1*) that lock the sensor proteins into a glucose-bound conformation and cause constitutive, glucose-independent expression of *HXT* genes (21) (Fig. 4A). We examined the stability of the active forms of the glucose sensors by Western blotting and found that, compared with wild type glucose sensors, both Rgt2-1 and Snf3-1 sensors remain stable regardless of glucose concentration (Fig. 4, B and C). It was also noted that low levels of Snf3-1-HA in glucose-grown cells (Fig. 4C, *High*) may be due to glucose repression of *SNF3* gene expression (Fig. 2).

We also examined whether the degradation-resistant glucose sensor mutants (Rgt2-1 and Snf3-1) can generate a signal even in the absence of glucose that leads to constitutive expression of *HXT* genes. Rgt2 is required for high glucose induction of *HXT1* expression, and Snf3 is required for low glucose induction of *HXT2* expression (21). Accordingly, we expressed Rgt2-1 and Snf3-1 in *HXT1*-NAT and *HXT2*-NAT reporter strains, respectively, in which the NAT (nourseothricin) resistance gene is expressed under the control of the *HXT* promoters (36). Colony assays showed that expression of Rgt2-1-HA or GFP-Rgt2-1 sensor allows the yeast cells to grow equally well in

medium containing different concentrations of glucose (Fig. 4D).

Snf3-1 is resistant to degradation, but its expression is repressed by glucose (Fig. 4C). Therefore, we observed that glucose repression of *SNF3* gene expression leads to the poor growth phenotype of the *HXT2*-NAT reporter strain expressing Snf3-1-HA (Fig. 4E, *Snf3-1-HA, Glu*) and that, by contrast, expression of GFP-Snf3-1, whose expression is not regulated by glucose, enables the reporter strain to grow on glucose (Fig. 4E, *GFP-Snf3-1, Glu*). These results reinforce the view that Snf3 expression is regulated at both transcriptional and post-translational levels (Fig. 2).

Consistently, confocal microscopy demonstrated that Rgt2-1 and Snf3-1 glucose sensors, compared with wild type Rgt2 and Snf3 sensors, accumulate at the plasma membrane, regardless of glucose concentration (Fig. 4F). These results suggested that conformation of the glucose sensors may be critical for their stability.

Signaling Defective Rgt2 Mutant Is Constitutively Targeted for Vacuolar Degradation—To corroborate our hypothesis that glucose sensors may be stable in their glucose-bound, signaling state, we examined the stability of signaling defective glucose sensors against degradation. The yeast galactose transporter Gal2 can recognize both galactose and glucose, and Phe⁵⁰⁴ of Gal2, which corresponds to Trp⁵²⁹ of Rgt2, is critical for sub-

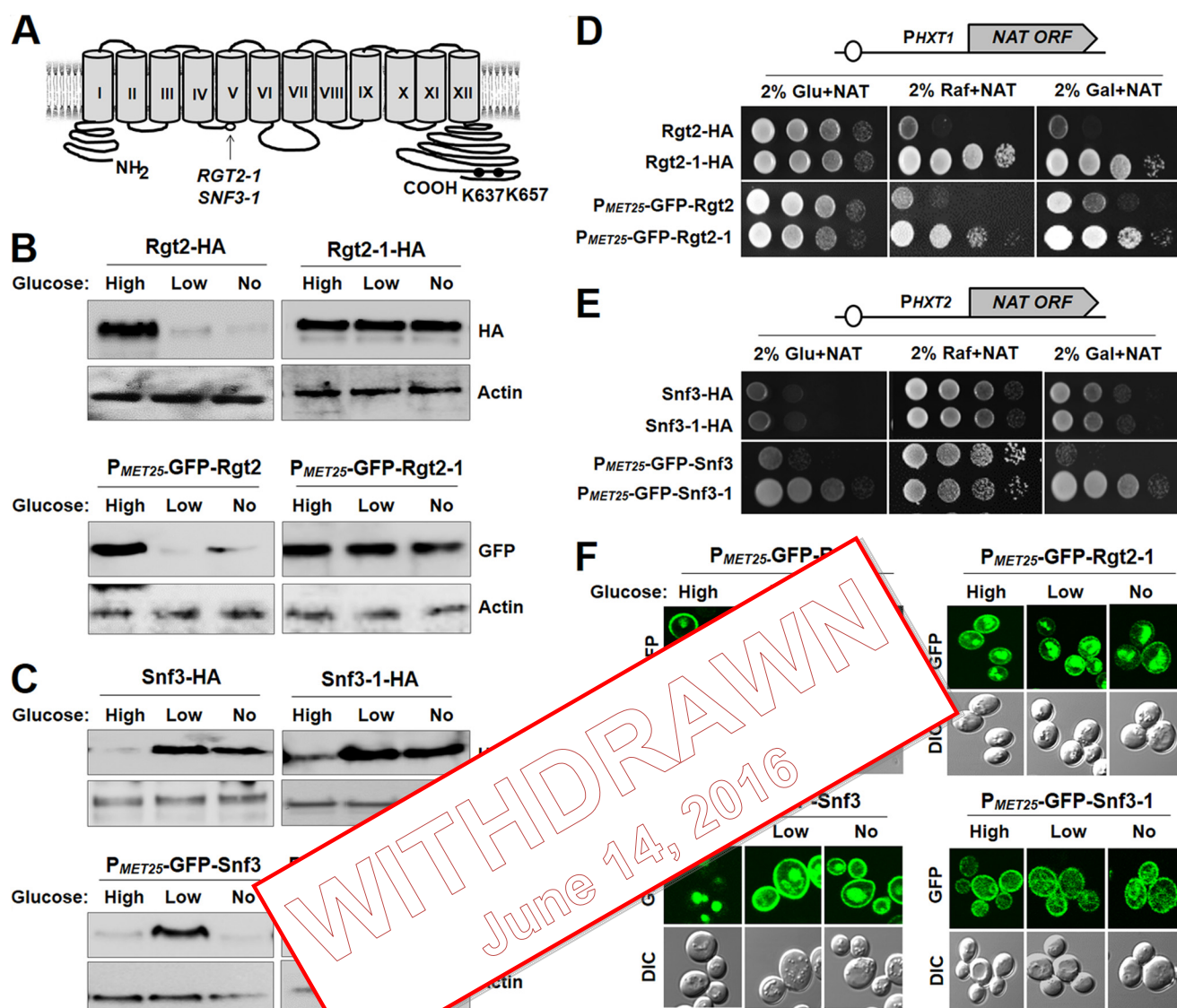


FIGURE 4. Constitutively active Rgt2-1 and Snf3-1 glucose sensors do not undergo endocytosis. A, a schematic diagram of the predicted secondary structure of the Rgt2 glucose sensor showing 12 transmembrane domains, cytoplasmic N- and C-terminal tails, two constitutive mutations (*RGT2-1* (R231K) and *SNF3-1* (R229K)), and two putative ubiquitin-acceptor lysine residues (Lys⁶³⁷ and Lys⁶⁵⁷). B and C, yeast cells (WT) expressing the indicated Rgt2 proteins (B) or Snf3 proteins (C) were grown in glucose (High), raffinose (Low), or galactose (No) medium, and membrane fractions were immunoblotted with anti-HA or anti-GFP antibody. Actin served as a loading control. GFP fusions of glucose sensors (GFP-Rgt2, GFP-Rgt2-1, GFP-Snf3, and GFP-Snf3-1) were expressed from the *P_{MET25}* promoter. D, the *P_{HXT1}*-NAT reporter strain (JKY88) expressing the indicated Rgt2 proteins was spotted on SC-2% glucose (*Glu*), SC-2% raffinose (*Raf*), or SC-2% galactose (*Gal*) plates supplemented with 100 μ g/ml NAT sulfate. The first spot of each row represents a count of 5×10^7 cell/ml, which is diluted 1:10 for each spot thereafter. The glucose plates and the galactose and raffinose plates were incubated for 2 and 3 days, respectively. E, the *P_{HXT2}*-NAT reporter strain (JKY89) expressing the indicated Snf3 proteins was spotted and photographed as described for D. F, yeast cells (WT) expressing GFP-Rgt2, GFP-Rgt2-1, GFP-Snf3, and GFP-Snf3-1 were grown as described above (B and C) and analyzed by confocal microscopy.

strate recognition (37). We replaced Trp at position 529 with aromatic amino acids Phe and Tyr using site-directed mutagenesis and determined the stability of the resulting Rgt2 mutants Rgt2^{W529F} and Rgt2^{W529Y} in high glucose-grown cells. The results showed that, in contrast to wild type Rgt2, the mutant Rgt2 sensors, Rgt2^{W529Y} in particular, was endocytosed and degraded even in the presence of glucose (Fig. 5A), leading to inhibition of the glucose induction of *HXT1* gene expression (Fig. 5B). Thus, Rgt2^{W529Y} was not able to complement the growth defect of the *rgt2snf3* double mutant in glucose medium (Fig. 5C). High glucose-induced proteasomal degradation of Mth1 is triggered by glucose activation of the Rgt2 sensor (14, 16). Western blot analysis showed that glucose-dependent

Mth1 degradation occurs in cells expressing the wild type Rgt2 sensor but not the Rgt2^{W529Y} sensor (Fig. 5D). These observations support the view that the stability of the glucose sensors may be determined by their ability to sense glucose.

DISCUSSION

Many yeast nutrient receptors and transporters, such as Zrt1 (38), Ctr1 (35), Fth1 (39), Smf1 (40), Fur4 (24), and Gap1 (31), are regulated in a homeostatic fashion. They are induced in the absence of their ligands but internalized and targeted for degradation in the vacuole when their ligands become available in excess (25, 26). Hence, endocytic degradation of these plasma membrane proteins functions as a homeostatic regulatory loop

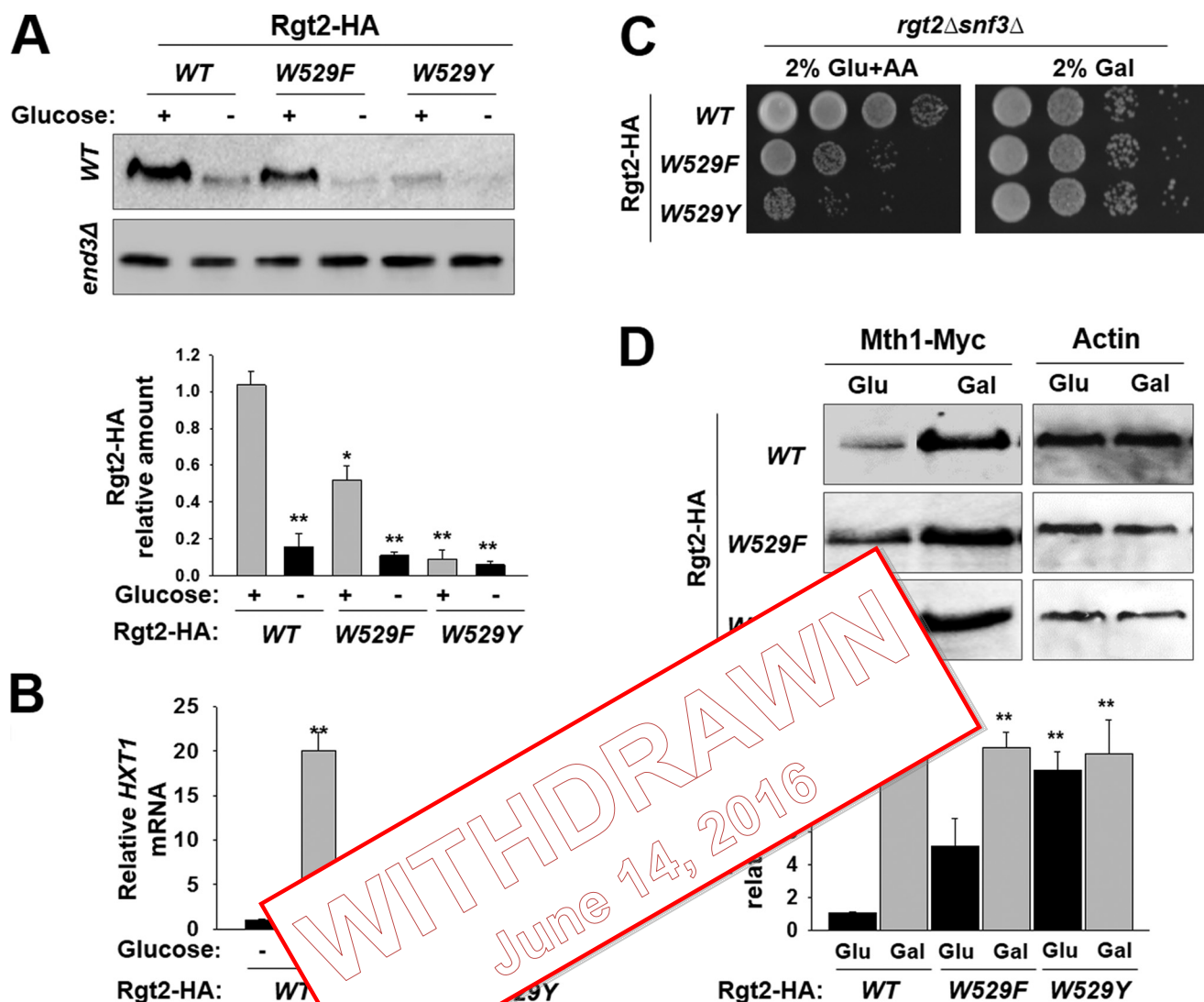


FIGURE 5. Signaling defective Rgt2 glucose sensors are constitutively endocytosed. *A*, yeast cells (WT and *end3Δ*) expressing the indicated Rgt2-HA proteins were grown as described for Fig. 1*F*, and membrane fractions were immunoblotted with anti-HA antibody (top panels). The intensity of each band on the blot was quantified by densitometric scanning (bottom panel; *, $p < 0.05$; **, $p < 0.001$). *B*, yeast cells (*rgt2Δsnf3Δ*) expressing the indicated Rgt2-HA proteins were grown as described for Fig. 3*C*, and the mRNA levels of *HXT1* were quantified by qRT-PCR. The values shown are means \pm S.D. (*, $p < 0.05$; **, $p < 0.001$). *C*, yeast cells (*rgt2Δsnf3Δ*) expressing the indicated Rgt2-HA proteins were spotted on 2% glucose plate supplemented with antimycin A (1 μ g/ml) (2% Glu + AA) or SC-2% galactose plate (2% Gal) and photographed as described for Fig. 4*D*. *D*, yeast cells (*rgt2Δsnf3Δ*) coexpressing Mth1-Myc and the indicated Rgt2-HA proteins were grown as described for Fig. 1*F*, and cell lysates were immunoblotted with anti-Myc antibody (top left panels, Mth1-Myc). Actin was served as a loading control (top right panels, actin). Quantification data of Mth1-Myc protein by densitometry are shown (bottom panel; *, $p < 0.05$; **, $p < 0.001$).

to prevent excessive ligand-induced activation of downstream effectors (41, 42). By contrast, we show here that the glucose sensors undergo endocytosis and vacuolar degradation in the absence of their ligand glucose. Of note, the stability of the Rgt2 and Snf3 glucose sensors at the plasma membrane is correlated with their ability to sense glucose, leading to the view that the actively signaling state of glucose sensors is protected from degradation.

This view is supported by the findings that the conformation of the glucose receptors determines their stability (Fig. 4). The *RGT2-1* or *SNF3-1* mutation has been postulated to lock the glucose sensor in a glucose-bound, signaling form, leading to the hypothesis that glucose binding to the glucose sensors suffices to initiate signaling (20, 21, 43). The constitutively active glucose sensor Rgt2-1 (Rgt2^{R231K}) and Snf3-1 (Snf3^{R229K}) do not undergo endocytosis and accumulate at the cell surface

regardless of glucose concentration. We also identify an *RGT2* mutation that converts Rgt2 sensor to a constitutively inactive form and show that this signaling defective Rgt2 mutant (Rgt2^{W529Y}) is constitutively targeted to the vacuole for degradation (Fig. 5). Glucose binding likely induces a series of structural changes in glucose sensors and transporters. Glucose transporters may undergo a conformational change upon glucose binding from the outward facing, signaling conformation to the inward facing, nonsignaling conformation that allows glucose to be released inside the cell; in contrast, the glucose sensors cannot switch to the inward facing conformation (44). The nature of *RGT2* W529Y mutation is not well understood, but we surmise that the Rgt2 mutant (Rgt2^{W529Y}) may not be able to sense glucose or to be converted into the outward facing, signaling conformation after binding to glucose.

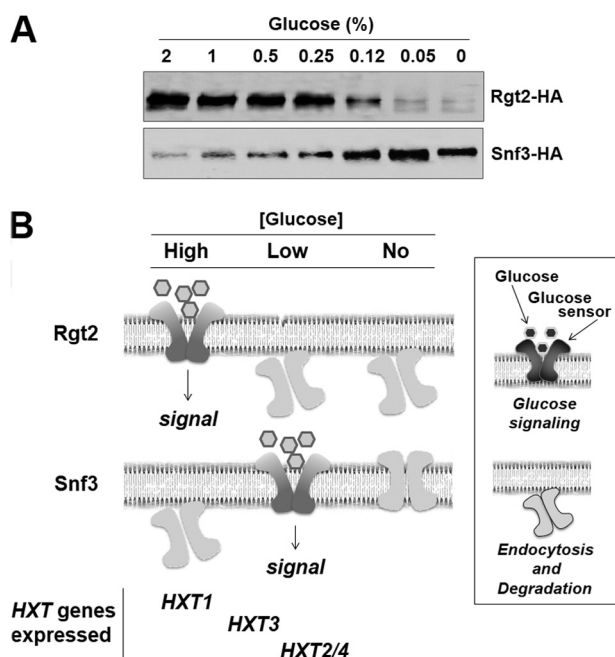


FIGURE 6. The turnover of the glucose sensors plays an important role in the adaptation to changing glucose levels. A, a comparison of the amounts of Rgt2-HA and Snf3-HA at the plasma membrane in cells grown in different glucose concentrations is shown (adapted from Figs. 1A and 2A). The first through seventh lanes denote different concentrations of glucose (% w/v): 2, 1, 0.5, 0.25, 0.125, 0.05, and 0, respectively. B, stability of the glucose sensors is associated with their ability to sense glucose. The low affinity glucose sensor Rgt2 is endocytosed and targeted to the vacuole for degradation in glucose-starved cells but is stable in cells grown in high glucose medium. The high affinity glucose sensor Snf3 is regulated at both the transcriptional and posttranslational levels: Snf3 is internalized and degraded in glucose-depleted high glucose-grown cells but also in glucose-depleted cells. Snf3 is also repressed by high glucose concentration. Consequently, Snf3 is stable in high glucose-grown cells. The turnover of the glucose sensors is a key mechanism for the transporters most appropriate for the environment.

The yeast cells cope with changing glucose availability by expressing at least six members of the hexose transporter family with different affinities for glucose (45–48). They express only those glucose transporters most appropriate for the amounts of glucose available in the environment (49). The glucose sensors have different roles in glucose signaling: the low affinity glucose sensor Rgt2 is responsible for expression of the low affinity glucose transporter Hxt1; the high affinity glucose sensor Snf3 regulates the expression of the high affinity glucose transporters Hxt2, Hxt3, and Hxt4 (21). This is consistent with our findings that Rgt2 is stable in high glucose grown cells, whereas Snf3, in cells grown on low glucose, reinforcing the view that the stability of the glucose sensors is correlated with their affinity for glucose. Moreover, the glucose sensors are localized to the vacuole regardless of the presence of glucose (Figs. 1F and 2E). These observations suggest that the glucose sensors may be inherently unstable but stabilized by glucose.

Our findings provide a conceptual framework to explain the regulation of glucose sensing activity at the yeast cell surface that directly affects the ability of the organism to adapt to fluctuating glucose levels. Glucose starvation induces endocytosis and degradation of Rgt2, and thus Rgt2 is stable in cells grown on high glucose. By contrast, Snf3 accumulates at the cell sur-

face of the cells grown on low glucose, mostly due to the regulation of Snf3 expression by both feedforward and feedback mechanisms. Snf3 protein is internalized and degraded not only in high glucose-grown cells but also in glucose-depleted cells, whereas expression of the *SNF3* gene is repressed by high glucose concentrations but is derepressed when glucose is absent (Fig. 2). We have previously shown that Mig1 and Mig2 repressors mediate glucose repression of *SNF3* gene expression (17, 28). Therefore, glucose-induced Snf3 degradation is reinforced by glucose repression of *SNF3* gene expression, but glucose depletion-induced Snf3 degradation is dampened by derepression of *SNF3* gene expression. As a result, substantial amounts of Snf3 are present at the cell surface of glucose-depleted cells (Fig. 2A). This should serve to provide for a rapid reestablishment of induction of *HXT* gene expression when glucose is available in the medium.

Consequently, one of the glucose sensors, or both, may be present at the plasma membrane at a given glucose concentration. Snf3 may be the predominant sensor in low levels of glucose and Rgt2, in high glucose conditions. Both Rgt2 and Snf3 may coexist in a cell, mediating the transition between high and low levels of glucose (Fig. 2). However, yeast cells can keep glucose sensors at the plasma membrane over a wide range of glucose concentrations, enabling them to respond rapidly to changes in glucose levels and thereby to maintain glucose homeostasis.

We thank Mark Johnston for providing plasmids and Christopher Burd for providing the *rsp5-1* mutant.

REFERENCES

1. Rolland, F., Wanke, V., Cauwenberg, L., Ma, P., Boles, E., Vanoni, M., de Winder, J. H., Thevelein, J. M., and Winderickx, J. (2001) The role of hexose transport and phosphorylation in cAMP signalling in the yeast *Saccharomyces cerevisiae*. *FEMS Yeast Res.* **1**, 33–45
2. Towle, H. C. (2005) Glucose as a regulator of eukaryotic gene transcription. *Trends Endocrinol. Metab.* **16**, 489–494
3. Ozcan, S., and Johnston, M. (1999) Function and regulation of yeast hexose transporters. *Microbiol. Mol. Biol. Rev.* **63**, 554–569
4. Holsbeek, I., Lagatie, O., Van Nuland, A., Van de Velde, S., and Thevelein, J. M. (2004) The eukaryotic plasma membrane as a nutrient-sensing device. *Trends Biochem. Sci.* **29**, 556–564
5. Johnston, M., and Kim, J. H. (2005) Glucose as a hormone. Receptor-mediated glucose sensing in the yeast *Saccharomyces cerevisiae*. *Biochem. Soc. Trans.* **33**, 247–252
6. Ozcan, S., Leong, T., and Johnston, M. (1996) Rgt1p of *Saccharomyces cerevisiae*, a key regulator of glucose-induced genes, is both an activator and a repressor of transcription. *Mol. Cell. Biol.* **16**, 6419–6426
7. Schmidt, M. C., McCartney, R. R., Zhang, X., Tillman, T. S., Solimeo, H., Wölfl, S., Almonte, C., and Watkins, S. C. (1999) Std1 and Mth1 proteins interact with the glucose sensors to control glucose-regulated gene expression in *Saccharomyces cerevisiae*. *Mol. Cell. Biol.* **19**, 4561–4571
8. Kim, J. H., Polish, J., and Johnston, M. (2003) Specificity and regulation of DNA binding by the yeast glucose transporter gene repressor Rgt1. *Mol. Cell. Biol.* **23**, 5208–5216
9. Kim, J. H. (2004) Immobilized DNA-binding assay, an approach for *in vitro* DNA-binding assay. *Anal. Biochem.* **334**, 401–402
10. Kim, J. H. (2009) DNA-binding properties of the yeast Rgt1 repressor. *Biochimie* **91**, 300–303
11. Kim, J. H., and Johnston, M. (2006) Two glucose-sensing pathways converge on Rgt1 to regulate expression of glucose transporter genes in *Sac-*

- Saccharomyces cerevisiae*. *J. Biol. Chem.* **281**, 26144–26149
12. Palomino, A., Herrero, P., and Moreno, F. (2006) Tpk3 and Snf1 protein kinases regulate Rgt1 association with *Saccharomyces cerevisiae* HXK2 promoter. *Nucleic Acids Res.* **34**, 1427–1438
13. Mosley, A. L., Lakshmanan, J., Aryal, B. K., and Ozcan, S. (2003) Glucose-mediated phosphorylation converts the transcription factor Rgt1 from a repressor to an activator. *J. Biol. Chem.* **278**, 10322–10327
14. Flick, K. M., Spielewoy, N., Kalashnikova, T. I., Guaderrama, M., Zhu, Q., Chang, H. C., and Wittenberg, C. (2003) Grr1-dependent inactivation of Mth1 mediates glucose-induced dissociation of Rgt1 from HXT gene promoters. *Mol. Biol. Cell* **14**, 3230–3241
15. Spielewoy, N., Flick, K., Kalashnikova, T. I., Walker, J. R., and Wittenberg, C. (2004) Regulation and recognition of SCFGrr1 targets in the glucose and amino acid signaling pathways. *Mol. Cell. Biol.* **24**, 8994–9005
16. Moriya, H., and Johnston, M. (2004) Glucose sensing and signaling in *Saccharomyces cerevisiae* through the Rgt2 glucose sensor and casein kinase I. *Proc. Natl. Acad. Sci. U.S.A.* **101**, 1572–1577
17. Kim, J. H., Brachet, V., Moriya, H., and Johnston, M. (2006) Integration of transcriptional and posttranslational regulation in a glucose signal transduction pathway in *Saccharomyces cerevisiae*. *Eukaryot. Cell* **5**, 167–173
18. Pasula, S., Chakraborty, S., Choi, J. H., and Kim, J. H. (2010) Role of casein kinase I in the glucose sensor-mediated signaling pathway in yeast. *BMC Cell Biol.* **11**, 17
19. Kim, J. H., Roy, A., Jouandot, D., 2nd, and Cho, K. H. (2013) The glucose signaling network in yeast. *Biochim Biophys. Acta* **1830**, 5204–5210
20. Ozcan, S., Dover, J., Rosenwald, A. G., Wölfl, S., and Johnston, M. (1996) Two glucose transporters in *Saccharomyces cerevisiae* are glucose sensors that generate a signal for induction of gene expression. *Proc. Natl. Acad. Sci. U.S.A.* **93**, 12428–12432
21. Ozcan, S., Dover, J., and Johnston, M. (1998) Glucose sensing and signaling by two glucose receptors in the yeast *Saccharomyces cerevisiae*. *J. Biol. Chem.* **273**, 2566–2573
22. Pasula, S., Jouandot, D., 2nd, and Kim, J. H. (2007) Regulation of glucose-independent induction of HXT expression in *Saccharomyces cerevisiae*. *FEBS Lett.* **581**, 3230–3234
23. Busti, S., Coccetti, P., Alberghina, I., and Johnston, M. (2009) Signaling-mediated coordination of glucose transport and metabolism in *Saccharomyces cerevisiae*. *Sensors* **10**, 619–630
24. Galan, J. M., Moreau, V., Andre, B., and Johnston, M. (1996) Ubiquitination mediated by the E3 complex is required for endocytosis of the yeast glucose transporter. *J. Biol. Chem.* **271**, 10946–10952
25. Kriel, J., Haesendonckx, S., Rubio-Tejada, L., Van Zeebroeck, G., and Thevelein, J. M. (2011) From transporter to transceptor. Signaling from transporters provokes re-evaluation of complex trafficking and regulatory controls. Endocytic internalization and intracellular trafficking of nutrient transporters may, at least in part, be governed by their signaling function. *Bioessays* **33**, 870–879
26. Rutherford, J. C., and Bird, A. J. (2004) Metal-responsive transcription factors that regulate iron, zinc, and copper homeostasis in eukaryotic cells. *Eukaryot. Cell* **3**, 1–13
27. Jouandot, D., 2nd, Roy, A., and Kim, J. H. (2011) Functional dissection of the glucose signaling pathways that regulate the yeast glucose transporter gene (HXT) repressor Rgt1. *J. Cell Biochem.* **112**, 3268–3275
28. Kaniak, A., Xue, Z., Macool, D., Kim, J. H., and Johnston, M. (2004) Regulatory network connecting two glucose signal transduction pathways in *Saccharomyces cerevisiae*. *Eukaryot. Cell* **3**, 221–231
29. Hicke, L., and Dunn, R. (2003) Regulation of membrane protein transport by ubiquitin and ubiquitin-binding proteins. *Annu. Rev. Cell Dev. Biol.* **19**, 141–172
30. Medintz, I., Jiang, H., and Michels, C. A. (1998) The role of ubiquitin conjugation in glucose-induced proteolysis of *Saccharomyces* maltose permease. *J. Biol. Chem.* **273**, 34454–34462
31. Springael, J. Y., and André, B. (1998) Nitrogen-regulated ubiquitination of the Gap1 permease of *Saccharomyces cerevisiae*. *Mol. Biol. Cell* **9**, 1253–1263
32. Amerik, A. Y., Nowak, J., Swaminathan, S., and Hochstrasser, M. (2000) The Doa4 deubiquitinating enzyme is functionally linked to the vacuolar protein-sorting and endocytic pathways. *Mol. Biol. Cell* **11**, 3365–3380
33. Rotin, D., Staub, O., and Hagenauer-Tsapir, R. (2000) Ubiquitination and endocytosis of plasma membrane proteins. Role of Nedd4/Rsp5p family of ubiquitin-protein ligases. *J. Membr. Biol.* **176**, 1–17
34. Gadura, N., and Michels, C. A. (2006) Sequences in the N-terminal cytoplasmic domain of *Saccharomyces cerevisiae* maltose permease are required for vacuolar degradation but not glucose-induced internalization. *Curr. Genet.* **50**, 101–114
35. Liu, J., Sitaram, A., and Burd, C. G. (2007) Regulation of copper-dependent endocytosis and vacuolar degradation of the yeast copper transporter, Ctr1p, by the Rsp5 ubiquitin ligase. *Traffic* **8**, 1375–1384
36. Roy, A., Shin, Y. J., and Kim, J. H. (2013) Construction of yeast strains useful for screening drugs that inhibit glucose uptake and glycolysis. *Anal. Biochem.* **436**, 53–54
37. Kasahara, T., and Johnston, M. (2000) Three aromatic amino acid residues critical for the function of the yeast Gal2 transporter. *J. Biol. Chem.* **275**, 4000–4004
38. Grollman, A. P., and Eide, D. (1998) Zinc transporter occurs through the yeast Gal2 transporter. *J. Biol. Chem.* **273**, 28617–28624
39. Grollman, A. P., Iwai, Y., Klausner, R. D., and Dancis, J. (1998) A complex involved in high-affinity iron uptake in yeast. *J. Biol. Chem.* **273**, 1552–1557
40. Grollman, A. P., and Culotta, V. C. (2009) Manganese homeostasis in *Saccharomyces cerevisiae*. *Chem. Rev.* **109**, 4722–4732
41. Grollman, A. P., and von Zastrow, M. (2008) Regulation of GPCRs by endocytosis and its potential implications. *Annu. Rev. Pharmacol. Toxicol.* **48**, 537–568
42. Sorkin, A., and von Zastrow, M. (2009) Endocytosis and signalling. Inter-twining molecular networks. *Nat. Rev. Mol. Cell Biol.* **10**, 609–622
43. Wu, B., Ottow, K., Poulsen, P., Gaber, R. F., Albers, E., and Kielland-Brandt, M. C. (2006) Competitive intra- and extracellular nutrient sensing by the transporter homologue Ssy1p. *J. Cell Biol.* **173**, 327–331
44. Van Zeebroeck, G., Bonini, B. M., Versele, M., and Thevelein, J. M. (2009) Transport and signaling via the amino acid binding site of the yeast Gap1 amino acid transceptor. *Nat. Chem. Biol.* **5**, 45–52
45. Boles, E., and Hollenberg, C. P. (1997) The molecular genetics of hexose transport in yeasts. *FEMS Microbiol. Rev.* **21**, 85–111
46. Reifengerger, E., Boles, E., and Ciriacy, M. (1997) Kinetic characterization of individual hexose transporters of *Saccharomyces cerevisiae* and their relation to the triggering mechanisms of glucose repression. *Eur. J. Biochem.* **245**, 324–333
47. Ko, C. H., Liang, H., and Gaber, R. F. (1993) Roles of multiple glucose transporters in *Saccharomyces cerevisiae*. *Mol. Cell. Biol.* **13**, 638–648
48. Kruckeberg, A. L. (1996) The hexose transporter family of *Saccharomyces cerevisiae*. *Arch. Microbiol.* **166**, 283–292
49. Ozcan, S., and Johnston, M. (1995) Three different regulatory mechanisms enable yeast hexose transporter (HXT) genes to be induced by different levels of glucose. *Mol. Cell. Biol.* **15**, 1564–1572

WITHDRAWN
June 14, 2016

Endocytosis and Vacuolar Degradation of the Yeast Cell Surface Glucose Sensors Rgt2 and Snf3

Adhiraj Roy and Jeong-Ho Kim

J. Biol. Chem. 2014, 289:7247-7256.

doi: 10.1074/jbc.M113.539411 originally published online January 22, 2014

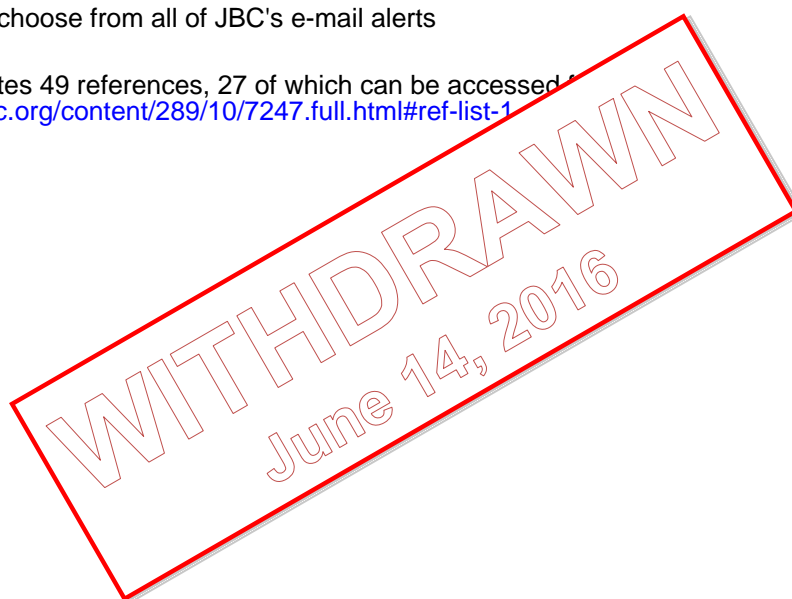
Access the most updated version of this article at doi: [10.1074/jbc.M113.539411](https://doi.org/10.1074/jbc.M113.539411)

Alerts:

- [When this article is cited](#)
- [When a correction for this article is posted](#)

[Click here](#) to choose from all of JBC's e-mail alerts

This article cites 49 references, 27 of which can be accessed at
<http://www.jbc.org/content/289/10/7247.full.html#ref-list-1>



Endocytosis and Vacuolar Degradation of the Yeast Cell Surface Glucose Sensors **Rgt2 and Snf3**

Adhiraj Roy and Jeong-Ho Kim

J. Biol. Chem. 2014, 289:7247-7256.

doi: 10.1074/jbc.M113.539411 originally published online January 22, 2014

Access the most updated version of this article at doi: [10.1074/jbc.M113.539411](https://doi.org/10.1074/jbc.M113.539411)

Alerts:

- [When this article is cited](#)
- [When a correction for this article is posted](#)

[Click here](#) to choose from all of JBC's e-mail alerts

This article cites 49 references, 24 of which can be accessed free at
<http://www.jbc.org/content/289/10/7247.full.html#ref-list-1>